

Measurement of the Gd-Gd exchange and dipolar interactions in $\text{Gd}_{0.01}\text{Y}_{0.99}\text{Ba}_2\text{Cu}_3\text{O}_6$

Ferenc Simon

Technical University of Budapest, Institute of Physics, P.O. Box 91, H-1521 Budapest, Hungary

Antal Rockenbauer

Chemical Research Center, Institute of Chemistry, P.O. Box 17, H-1525 Budapest, Hungary

Titusz Fehér and András Jánossy

Technical University of Budapest, Institute of Physics, P.O. Box 91, H-1521, Budapest, Hungary

Changkang Chen, Akhter J. S. Chowdhury, and Jonathon W. Hodby

Clarendon Laboratory, Parks Road, Oxford, United Kingdom

(Received 22 December 1998)

The microscopic parameters of the Gd-Gd pair interaction are measured in single crystals of the $\text{Gd}_{0.01}\text{Y}_{0.99}\text{Ba}_2\text{Cu}_3\text{O}_6$ cuprate using high-frequency (225 GHz) Gd^{3+} electron-spin resonance. In addition to the fine-structure spectrum of single Gd^{3+} ions, a series of low intensity resonance transitions are resolved at high magnetic fields and low temperatures which arise from Gd-Gd pairs. From the resonance line positions of nearest-neighbor Gd-Gd pairs we determine an isotropic exchange energy of $J=156$ mK and an anisotropic (mainly dipolar) interaction energy of $D=51.7$ mK. The anisotropic interaction parameters of second, third, and fourth neighbors correspond to the values expected for dipolar interaction only. [S0163-1829(99)02618-1]

I. INTRODUCTION

The magnetism of the rare-earth layers of the $\text{RBa}_2\text{Cu}_3\text{O}_{6+x}$ ($R123$, R =rare earth) perovskites has been intensively studied. In most cases these layers are well isolated from the sandwiching CuO_2 sheets. In $\text{Gd}123$, one of the most intensively investigated systems,¹⁻⁷ T_N , the antiferromagnetic ordering temperature of Gd depends little on the electronic state of the CuO_2 layers which may themselves be antiferromagnetic or superconducting. The Gd antiferromagnet is simple and it is tempting to derive the Néel temperature and the phase diagram of the magnetic structure from a few basic interactions: the single-ion anisotropy due to crystal fields (CF's), the first-neighbor isotropic exchange interaction, and anisotropic magnetic interactions between Gd^{3+} ions. The dipole-dipole (DD) interaction is probably the most important anisotropic pair interaction.

A precise knowledge of these parameters is still lacking. In this paper we determine the most important Gd^{3+} pair interaction parameters from high-frequency electron-spin resonance of $\text{Gd}_{0.01}\text{Y}_{0.99}\text{Ba}_2\text{Cu}_3\text{O}_{6+x}$ (small x) high-quality single crystals. The Gd concentration is low and we study essentially isolated paramagnetic Gd-Gd pairs surrounded by Y^{3+} ions. The Gd^{3+} electron-spin resonance lines are narrow and the lines of Gd-Gd near-neighbor pairs are resolved from the main line up to the fourth neighbor. The basic interaction parameters are determined independently from the analysis of the electron-spin-resonance (ESR) spectrum. The method is limited to high magnetic fields and low temperatures where only a small number of the low-lying energy levels of the various Gd-Gd pairs are populated and thus only a few, relatively intense transitions are observed. At higher temperatures or lower resonance fields many transitions appear and spectral intensities are too small for a useful analysis.

We review sample preparation and experimental procedures in Sec. II of this paper. Section III outlines the calcu-

lation of on-site CF, isotropic exchange and DD interactions from the observed ESR spectra. We present experimental results in Sec. IV. We analyze the experimental data, compare results with those in the literature using other techniques, and discuss their relevance to the magnetic Gd^{3+} sublattice of the $\text{Gd}123$ system in Sec. V.

II. SAMPLES AND EXPERIMENTAL DETAILS

In previous ESR experiments⁸ on the same crystals at temperatures above 20 K and at frequencies of 9, 75, 150, and 225 GHz were presented. The CF parameters and the g -factor anisotropy of Gd^{3+} ions with no near-neighbor pairs were determined. In this work we studied Gd^{3+} ESR in three single crystals of $\text{Gd}_{0.01}\text{Y}_{0.99}\text{Ba}_2\text{Cu}_3\text{O}_{6+x}$. The ESR spectra were the same for the three crystals, i.e., the same CF parameters and Gd-Gd pair-interaction parameters were found. All data presented in this paper correspond to a well-defined, triangular platelet with about 0.5 mm linear dimensions in the **(a,b)** ([001]) plane and 0.1 mm thick along **c**. The nominal 1% Gd concentration agrees with the observed ESR line-width, assuming this arises from Gd-Gd dipole interactions⁹ only. The as-grown single crystals were reduced at 800 °C in a dynamic vacuum for 72 h. This reduces the oxygen content of the Cu(1) plane to a few %. The Gd^{3+} ESR spectrum, itself a sensitive indicator of oxygen doping, was consistent with a low concentration of oxygen. In samples with $x > 0.15$ the variation of CF between Gd^{3+} sites with different numbers of Cu(1)-O chain neighbors splits each component of the Gd^{3+} fine structure into well-defined lines.¹⁰ No trace of oxygen chains has been detected in the ESR spectra of the present crystals.

We discuss ESR spectra recorded below 10 K and at 225 GHz for which the corresponding central transition Gd^{3+}

resonance field is at 8.1 T. All spectrometer functions and data collecting are computer controlled. The high-frequency spectrometer has a quartz stabilized Gunn diode source at 75 GHz followed by a frequency tripler. The sample is placed in a shorted waveguide and usually a linear superposition of derivative absorption and dispersion lines is detected. Audio modulation was used for lock-in detection. The spin-lattice relaxation rate of $\text{Gd}_{0.01}\text{Y}_{0.99}\text{Ba}_2\text{Cu}_3\text{O}_{6+x}$ is long with respect to the modulation frequency at low temperatures and the line shape is affected by saturation effects.

The high population of the lowest-lying energy levels in high magnetic fields and low temperatures facilitates the observation and assignment of dipolar satellites.¹¹ Transient effects further enhance the observed amplitude below 10 K. We have not understood this amplitude enhancement which occurs when spin-lattice relaxation becomes slower than the audio modulation frequency. In the spectrometer the radiation reflected from the sample is mixed with a reference mm wave field to detect the absorption and dispersion components of the ESR separately. At low temperatures and moderately high modulation frequencies (typically 10 kHz) the line shape is nearly independent of the phase of the reference mm wave radiation. The observed lines resemble fast passage spectra of paramagnetic centers in solids.¹² In the fits we approximated this line shape by a (nonderivative) Lorentzian absorption. Transition intensities and shapes were of little importance for the fit since the interaction parameters are derived from the position of lines. In the high-quality single crystals, lines are narrow and are slightly broadened only by strains or impurities and line positions could be determined accurately.

III. METHOD TO DETERMINE THE BASIC INTERACTION PARAMETERS

The spin Hamiltonian of two Gd^{3+} ions interacting on neighboring lattice sites is

$$H(\mathbf{S}_1, \mathbf{S}_2) = H_{z1}(\mathbf{S}_1) + H_{z2}(\mathbf{S}_2) + H_{c1}(\mathbf{S}_1) + H_{c2}(\mathbf{S}_2) + H_{\text{ex}}(\mathbf{S}_1, \mathbf{S}_2) + H_{\text{dip}}(\mathbf{S}_1, \mathbf{S}_2). \quad (1)$$

\mathbf{S}_1 and \mathbf{S}_2 denote the $4f^7$ electron spin-operators of the two Gd^{3+} ions. H_{z1} , H_{z2} are the Zeeman Hamiltonians of the two Gd^{3+} ions. H_{c1} and H_{c2} stand for the corresponding on-site CF Hamiltonians. The two ions are coupled by the H_{ex} , exchange and H_{dip} , DD interaction terms. In the high-field ESR technique the Zeeman energy is the largest interaction and we index the energy levels and transitions by the Zeeman eigenvalues $|S_z\rangle$, $S_z = -7/2, \dots, +7/2$ of the nearly pure $^8S_{7/2}$ spin state of Gd^{3+} ions isolated from all other Gd^{3+} ions. The on-site tetragonal CF Hamiltonian is

$$H_{\text{tetra}} = 1/3 b_2^0 O_2^0 + 1/60 b_4^0 O_4^0 + 1/60 b_4^4 O_4^4 + 1/1260 b_6^0 O_6^0 + 1/1260 b_6^4 O_6^4. \quad (2)$$

We use O_m^n operator equivalents as defined in Ref. 13. The Gd^{3+} ions of a pair perturb each other and their CF differs from that of the isolated Gd^{3+} ions. The replacement of one of the Y^{3+} ions surrounding the Gd^{3+} ion by another Gd^{3+} breaks the tetragonal symmetry and further orthorhombic terms appear in Eq. (2) in addition to a change of the tetrag-

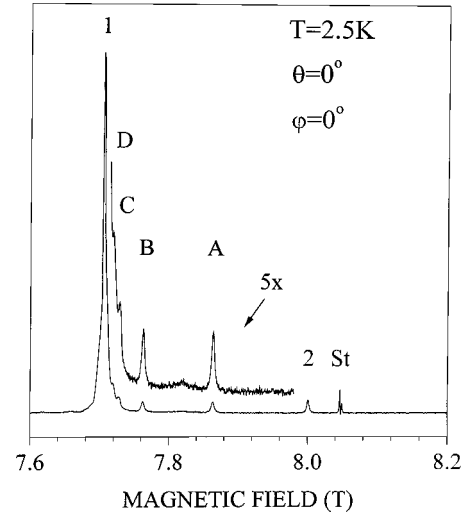


FIG. 1. Gd-Gd pair satellites in the Gd^{3+} ESR spectrum of $\text{Gd:YBa}_2\text{Cu}_3\text{O}_6$ for magnetic field $B \parallel c$. A, B, C, D are dipolar transitions of pairs with increasing separation. The transitions “1” and “2” are the isolated Gd^{3+} fine-structure lines $| -7/2 \rangle \rightarrow | -5/2 \rangle$ and $| -5/2 \rangle \rightarrow | -3/2 \rangle$, respectively. St is the magnetic-field calibration standard.

onal parameters. However, as long as this distortion is small, the orthorhombic terms have negligible effect on the ESR spectra for magnetic field along c .

We assume an isotropic Heisenberg exchange interaction

$$H_{\text{ex}}(\mathbf{S}_1, \mathbf{S}_2) = J \mathbf{S}_1 \mathbf{S}_2, \quad (3)$$

and the DD Hamiltonian in the point dipole approximation is

$$H_{\text{dip}} = D [\mathbf{S}_1 \mathbf{S}_2 - 3(\mathbf{S}_1 \mathbf{r})(\mathbf{S}_2 \mathbf{r})/r^2] \quad (4)$$

with $D = \mu_0 / (4\pi) (g_{\text{Gd}}^2 \mu_B^2) / r^3$. For the nearest-neighbor (NN) Gd^{3+} pairs (denoted by A) $D_A = 43$ mK in this approximation. [Gd^{3+} g factor is $g_{\text{Gd}} = 1.9871$ and $a = 3.8586 \text{ \AA}$ is the lattice constant of $\text{YBa}_2\text{Cu}_3\text{O}_{6.06}$ (Ref. 14)].

To describe the coupled system, we use states of the sum of the angular momentum $\mathbf{S} = \mathbf{S}_1 + \mathbf{S}_2$, $|S, M_S\rangle$ where $S = 0, \dots, 7$, $M_S = -S, \dots, S$. We use for convenience the direct product of the eigenvectors of the two isolated Gd^{3+} ions as a basis. We diagonalize the spin-Hamiltonian matrix to determine the eigenvectors and eigenvalues and the resonance fields as well as the transition amplitudes of the resonance transitions. Thermal population of the various energy levels is also taken into account.

IV. EXPERIMENTAL RESULTS ON Gd:Y123

A. Dipolar satellites independent of isotropic exchange

In addition to the normal Gd^{3+} fine structure, new resonance transitions appear at low temperatures (Fig. 1). We identify four satellite transitions (A, B, C, D) as dipolar satellites from interacting Gd^{3+} pairs. The dipole field of neighboring Gd^{3+} ions changes the local magnetic field and shifts the resonance. The point dipole approximation with pairs of Gd^{3+} ions at various distances [Fig. 2(a)] explains the data quite well. In a simple picture the satellite lines of Fig. 1 may be interpreted as transitions where one of the Gd^{3+} ions is excited from the $| -7/2 \rangle$ ground state to the first excited state

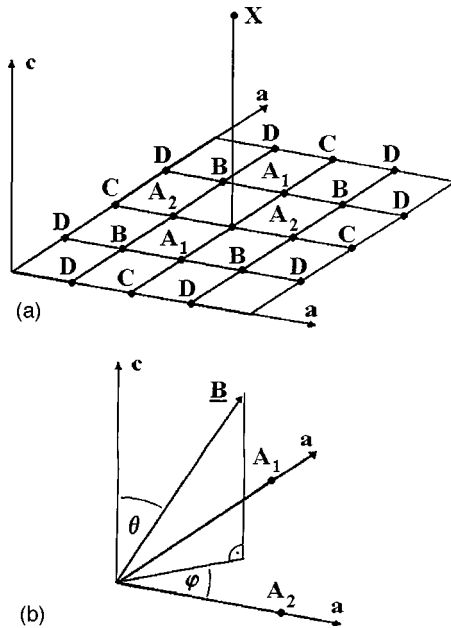


FIG. 2. (a) Sites of closest neighboring Gd³⁺ ions. A₁ and A₂ are in general inequivalent in arbitrarily oriented magnetic fields. (b) Definition of the polar coordinate system.

$| -5/2 \rangle$, while the neighboring ion remains in its ground state. In terms of the coupled system this is the $| 7, -7 \rangle \rightarrow | 7, -6 \rangle$ transition. The isotropic exchange does not affect this transition. The position of satellites *with respect to the main line* was calculated from Eq. (4). [The main lines follow the angular dependence given by Eq. (2).]

In an arbitrary oriented magnetic field, pairs like A₁ and A₂ of Fig. 2(a) are not equivalent. Figure 3 shows typical spectra at various magnetic-field orientations defined in the coordinate system of Fig. 2(b). As expected, the nearest-neighbor (NN) satellite A is clearly split even for small rotations θ of the magnetic field from the [001] direction towards the [100] direction. For a magnetic field along [100] A₁ and A₂ are split by several hundred mT. Rotations around [110] do not split satellite A. On the other hand, the next-nearest-neighbor satellite B, is broadened for a small rotation around [110] and is unaffected for rotations around [100]. For magnetic field along [100] the spectrum is complicated, a large number of dipolar satellites appear around the main transition, and an unambiguous assignment of all lines is difficult.

The first resonance transitions from excited states of Gd³⁺ pairs appear above 5 K (Fig. 4). Above 10 K the amplitude of the satellites decreases rapidly and with the appearance of a large number of transitions between higher energy levels the satellite spectrum becomes complicated. In the following we discuss the spectra observed between 5 and 10 K. The schematic energy-level diagram of the low-lying states is shown in Fig. 5. A dipolar pattern similar to that of transition “1” emerges for fine-structure line “2” which is due to the $| 6, -6 \rangle \rightarrow | 6, -5 \rangle$ transitions of the various neighbors. The NN neighbor line A' is well resolved. The shift, 169.0 mT, of the A' transition from the fine-structure line 2, differs somewhat from the shift of the A transition from transition 1 (154.5 mT). This implies that the shifts are not only from dipolar fields but the tetragonal crystal-field parameters of a NN Gd³⁺ pair and an isolated Gd³⁺ ion are also different.

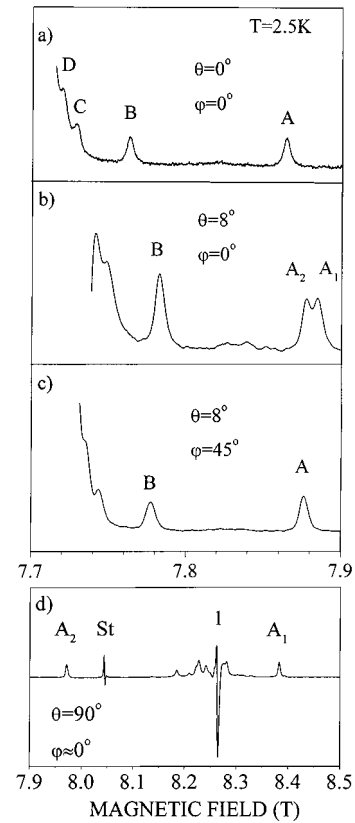


FIG. 3. Dependence of Gd-Gd pair satellites on the orientation of magnetic field.

B. Isotropic exchange dependent satellite transition

Above 5 K a further line, denoted by A*, appears (Fig. 4). We assign this to the $| 6, -6 \rangle \rightarrow \alpha | 7, -5 \rangle + \beta | 5, -5 \rangle$ transition of a NN pair which depends on the isotropic exchange interaction between the NN Gd³⁺ ions (Fig. 5). The isotropic exchange interaction shifts the initial and final states of the allowed $\Delta S=0$, $\Delta M_S=1$ transitions equally, therefore the frequencies of the $| 7, -7 \rangle \rightarrow | 7, -6 \rangle$ and $| 6, -6 \rangle \rightarrow | 6, -5 \rangle$ transitions (lines A and A') are unaffected by the isotropic

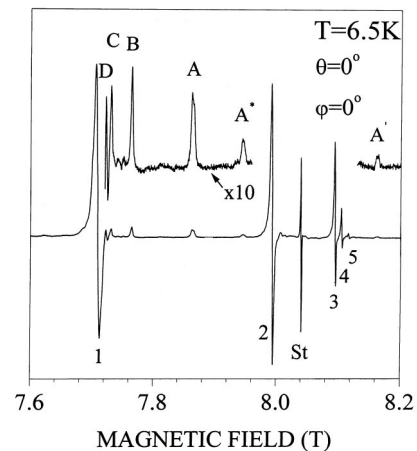


FIG. 4. Gd-Gd pair satellites at higher temperatures. The transition A* is used to measure the isotropic exchange interaction. The 1, 2, 3, 4, 5 transitions are the $| -7/2 \rangle \rightarrow | -5/2 \rangle$, $| -5/2 \rangle \rightarrow | -3/2 \rangle$, etc., fine-structure lines of isolated Gd³⁺.

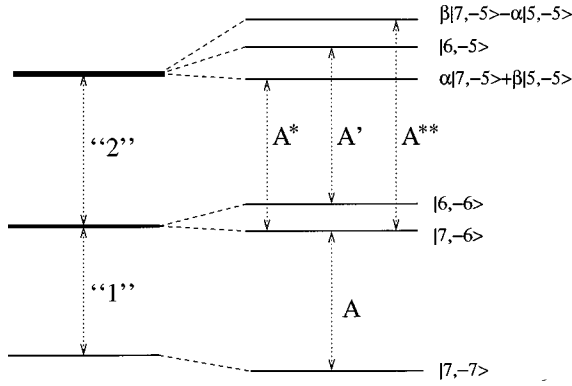


FIG. 5. Energy-level scheme of an interacting Gd-Gd pair. The transitions A and A' are independent of J while A^* and A^{**} depend on J .

exchange interaction. On the other hand, the degeneracy of the $|7, -5\rangle$, $|6, -5\rangle$, and $|5, -5\rangle$ Zeeman levels of the coupled Gd pair is lifted by the CF, DD, and isotropic exchange interactions and the $|7, -5\rangle$, $|5, -5\rangle$ states are mixed. Consequently, the otherwise forbidden A^* , A^{**} transitions which depend on the exchange interaction become observable.

We assign the line A^* to the $|7, -6\rangle \rightarrow \alpha|7, -5\rangle + \beta|5, -5\rangle$ transition for the following reasons. The intensity of transition A^* increases with temperature just like the NN dipolar satellite A' as expected if the exchange and dipolar energies are small compared to the Zeeman energy [Figs. 6(a) and 6(b)]. For magnetic fields along $[001]$ the shift of A^* from the fine-structure line "2", $\Delta = -48.0$ mT, is large and negative. Thus A^* cannot arise from a $|6, -6\rangle \rightarrow |6, -5\rangle$ transition of a Gd neighbor in the same

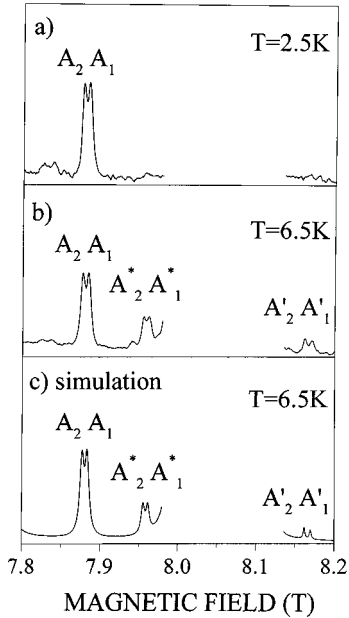


FIG. 6. (a) and (b) Assignment of A^* of Fig. 5 to the NN Gd pair satellite. Magnetic-field orientation: $\theta = 8^\circ$, $\varphi = 0^\circ$. A^* splits the same way as A and A' , and with increasing temperature A^* grows together with the A' transition. (c) Simulation of the ESR spectrum using the optimized parameters and (nonderivative) absorption Lorentzian line shapes. The main transition "2" at 8.05 T is omitted for clarity.

TABLE I. Calculated dipolar fields, $3/2DS/g\mu_B$, ($S = -7/2$) and measured shifts of the resonance lines of various neighbors, $\mathbf{B}||c$.

Dipole satellite	Calculated dipolar field (mT)	Shift from transition 1 (mT)
A [100]	-168.3	154.5
B [110]	-59.5	55.0
C [200]	-21.0	21.5
D [210]	-15.2	15.5

CuO_2 sandwich since these have positive shifts. The neighbor X in the sandwich above [Fig. 2(a)] has a satellite with a negative shift of only -12 mT and cannot be assigned to A^* . (The dipolar satellites of the X neighbor and other nearby sites appear as a shoulder at the low-field side of the fine-structure lines.) The A^* transition appears only above 5 K and this rules out that it is from Gd^{3+} ions near defects or other impurities. In that case a further line corresponding to excitations from the ground state would be observed which would be stronger than A^* at low temperatures. We have not seen any transition with the expected intensity within a broad magnetic-field sweep (between 0 and 9 T). Similar arguments exclude that transition A^* arises from a paramagnetic impurity (e.g., Gd^{3+} at an unusual site). The A^* transition was observed at orientations with \mathbf{B} slightly tilted from the c axis also. The A^* transition has the same angular dependence as the A and A' transitions [Figs. 4 and 6(b)]. The dipolar interaction of the inequivalent NN Gd^{3+} ions accounts for the splitting of A^* . We did not observe the A^* transition for \mathbf{B} in the $[001]$ plane. This agrees with the assignment, where our calculation predicts a negligible transition amplitude when \mathbf{B} is in the $[001]$ plane. We did not observe the A^{**} , $|6, -6\rangle \rightarrow \beta|7, -5\rangle - \alpha|5, -5\rangle$ transition, it is expected to have small intensity and is shifted above 9 T.

V. DISCUSSION

A. Analysis of experimental data

The dipolar interaction data of Table I represent a first approximation in which the crystal field is assumed to be the same for pairs and for the single ions. The measured shifts of the satellite resonance fields follow the calculated dipolar fields. This approximation is better for far lying neighbors, B, C, D than for the first neighbor A . We made a more precise analysis for pair A and values of the isotropic exchange constant J , the NN point dipole parameter D_A and the CF parameter b_2^0 are summarized in Table II. These parameters were determined from observed positions of A, A^*, A' (or $A_1, A_2, A_1^*, A_2^*, A_1', A_2'$ for orientations where \mathbf{B} was tilted from c and the splitting of lines was resolved). The exact orientation of the crystal with respect to the magnetic field, angles θ and φ , were determined from the main lines, i.e., from the single-ion Gd^{3+} fine structure.⁸ We took into account the anisotropy of the g factor⁸ also. We optimized all parameters simultaneously using several spectra with θ less than 12° . A typical simulated spectrum is shown in Fig. 6(c). Agreement between measured and calculated line positions is better than 1/3 of the linewidth for all lines.

TABLE II. Microscopic parameters of the NN Gd-Gd pairs.

	Crystal field b_2^0 (mK)	Isotropic exchange (J) (mK)	Dipolar and anisotropic exchange (D_A) (mK)	Calculated point dipole (mK)
Nearest-neighbor	-71.0 ± 1	156 ± 10	51.7 ± 1	43
Single Gd^{3+} (Ref. 8)	-57.3			

B. Comparison with other experiments

Following the discovery of antiferromagnetism in Gd123, there were a number of attempts to measure the value of the Gd-Gd exchange interaction. We list some of these measurements for various oxygen and Gd concentrations. The Néel temperature and thus the exchange interaction does not vary much with oxygen concentration.

Estimated values of J in $\text{Gd}_y\text{Y}_{1-y}\text{Ba}_2\text{Cu}_3\text{O}_{6+x}$ (Refs. 2 and 5) and in $\text{GdBa}_2\text{Cu}_3\text{O}_{6+x}$ (Refs. 1, 3, 6, 7) depend on the method used and the approximations involved. For example, Kikuchi *et al.*¹ and Nakamura *et al.*² inferred J values of 100 and 181 mK, respectively, from the Gd^{3+} ESR linewidth in the paramagnetic state. Filip *et al.*⁵ included crystal fields in their analysis of the Gd^{3+} linewidth and deduced $J = 70$ mK. Other methods involve the field-induced magnetization $M(B)$ in the ordered state. Le Dang *et al.*³ deduced $J = 50$ mK in $\text{GdBa}_2\text{Cu}_3\text{O}_7\text{H}_{1.55}$ from $M(B)$ but they neglected anisotropic interactions. A magnetic-field-temperature phase diagram of Gd123 was deduced by Djakonov *et al.*⁶ from static magnetization measurements of a single crystal at low temperatures. The phase diagram allows the determination of both isotropic and anisotropic interactions and a value of $J = 35$ mK was found.⁶ Nehrke and Pieper⁷ proposed $J = 72$ mK from NMR of the magnetic Cu(2) sites and a rather different phase diagram than that of Djakonov *et al.*

We believe that our result of $J = 156$ mK is more reliable than the above values since we measure the anisotropic (dipolar) and isotropic exchange interactions for the first-neighbor Gd-Gd pair and the crystal field at the Gd^{3+} site independently and with a high precision. The data of Table II may serve to construct a magnetic phase diagram of Gd123 if it is assumed that the pair interactions are the same as in dilute Gd:Y123 and that next-neighbor interactions are negligible. Parameters of an isolated Gd pair and those of the Gd123 compound are unlikely to differ very much. The lattice parameters of Gd:Y123 differ by about 1% from those of

Gd123 and the first-neighbor dipolar interactions differ by the same order of magnitude. The exchange interaction is probably insensitive to such small changes also. Although the CF parameters of Gd^{3+} ions in Gd123 have not been determined directly it is unlikely that they differ much from those of isolated Gd^{3+} . The CF is determined by the close surroundings of the Gd site. The valence of Gd^{3+} and Y^{3+} ions is the same and the change in the CF arises only from the variation of the lattice constants.

VI. CONCLUSIONS

We have measured the high-field ESR spectra of insulating $\text{Gd}_{0.01}\text{Y}_{0.99}\text{Ba}_2\text{Cu}_3\text{O}_{6+x}$ single crystals with x near zero. A series of low intensity lines were observed and assigned to transitions between Zeeman levels of exchange and dipolar coupled pairs of Gd^{3+} moments. From the resonance line positions we determined the strength of the isotropic exchange and anisotropic interactions between the moments of the NN pairs and the change of the crystal-field parameter b_2^0 relative to isolated Gd^{3+} ions. The measured isotropic exchange interaction $J = 156$ mK agrees reasonably with estimates in the literature but we believe our method is more reliable since the exchange, dipolar and crystal-field interactions can be readily separated in the ESR spectra of single crystal at low temperatures. We argue that the parameters measured for the NN Gd pair embedded in Y are not much different from those in the antiferromagnetic Gd123 compound and thus may serve as a basis to derive the magnetic phase diagram.

ACKNOWLEDGMENTS

Support by Hungarian state Grant Nos. OTKA T015984 and FKFP 0352/1997 and by the E.P.S.R.C for the National Crystal Growth Facility for Superconducting Oxides at Oxford is gratefully acknowledged.

¹H. Kikuchi, Y. Ajiro, Y. Ueda, K. Kosuge, M. Takano, Y. Takeda, and M. Sato, *J. Phys. Soc. Jpn.* **57**, 1887 (1988).

²F. Nakamura, Y. Ochiai, H. Shimizu, and Y. Narahara, *Phys. Rev. B* **42**, 2558 (1990).

³K. Le Dang, J. P. Renard, P. Veillet, and E. Vélú, *Phys. Rev. B* **40**, 11 291 (1989).

⁴D. McK. Paul, H. A. Mook, A. W. Hewat, B. C. Sales, L. A. Boatner, J. R. Thompson, and M. Mostoller, *Phys. Rev. B* **37**, 2341 (1988).

⁵C. Filip, C. Kessler, F. Balinbanu, A. Darabont, L. V. Giurgiu,

and M. Mehring, *Physica C* **235**, 1645 (1994).

⁶V. P. Djakonov, E. E. Zubov, L. P. Kozeeva, G. G. Levchenko, V. I. Makrovich, A. D. Pavlyuk, and I. M. Fita, *Physica C* **178**, 221 (1991); M. Baran, V. P. Dyakonov, I. M. Fita, G. G. Levchenko, V. I. Marchenkov, E. E. Zubov, and H. Szymczak, *ibid.* **245**, 257 (1995).

⁷K. Nehrke and M. W. Pieper, *Phys. Rev. B* **51**, 12 618 (1995).

⁸A. Jánossy, F. Simon, T. Fehér, A. Rockenbauer, L. Korecz, C. Chen, A. J. S. Chowdhury, and J. W. Hodby, *Phys. Rev. B* **59**, 1176 (1999).

- ⁹A. Jánossy, A. Rockenbauer, and S. Pekker, *Physica C* **167**, 301 (1990).
- ¹⁰S. Pekker, A. Jánossy, and A. Rockenbauer, *Physica C* **181**, 11 (1991).
- ¹¹A. Rockenbauer, T. Fehér, A. Jánossy, and J. Hodby, 28th Congress Ampere, Extended Abstracts, edited by M. E. Smith and J. H. Strange, University of Kent at Canterbury, 1996, pp. 189–190.
- ¹²A. Abragam, *The Principles of Nuclear Magnetism* (Clarendon, Oxford, 1962).
- ¹³A. Abragam and B. Bleaney, *Electron Paramagnetic Resonance of Transition Ions* (Clarendon, Oxford, 1970).
- ¹⁴J. M. Tranquada, A. H. Moudden, A. I. Goldman, P. Zolliker, D. E. Cox, G. Shirane, S. K. Sinha, D. Vaknin, D. C. Johnston, M. S. Alvarez, A. J. Jacobson, J. T. Lewandowski, and J. M. Newsam, *Phys. Rev. B* **38**, 2477 (1988).